HHS Public Access

Author manuscript

Nat Neurosci. Author manuscript; available in PMC 2013 February 01.

Published in final edited form as:

Nat Neurosci. ; 15(8): 1117–1119. doi:10.1038/nn.3153.

Corticostriatal functional connectivity predicts transition to chronic back pain

Marwan N. Baliki[1], **Bogdan Petre**[1], **Souraya Torbey**[1], **Kristina M. Herrmann**[1], **Lejian Huang**[1], **Thomas J. Schnitzer**[2], **Howard L. Fields**[3], and **A. Vania Apkarian**[1,4,*]

[1]Department of Physiology, Northwestern University, Feinberg School of Medicine, Chicago, Illinois, 60611, USA

[2]Department of Rheumatology, Northwestern University, Feinberg School of Medicine, Chicago, Illinois, 60611, USA

[3]Department of Neurology and The Ernest Gallo Clinic & Research Center, University of California, San Francisco, 5858 Horton Street, Suite 200, Emeryville, California 94608, USA

[4]Departments of Anesthesia and Surgery, Northwestern University, Feinberg School of Medicine, Chicago, Illinois, 60611, USA

Abstract

The mechanism of brain reorganization in pain chronification is unknown. In a longitudinal brain imaging study, sub–acute back pain (SBP) patients were followed over one year. When pain persisted (SBPp, in contrast to recovering SBP, and healthy controls), brain gray matter density decreased. Importantly, initially greater functional connectivity of nucleus accumbens with prefrontal cortex predicted pain persistence, implying that corticostriatal circuitry is causally involved in the transition from acute to chronic pain.

Although human brain imaging studies demonstrate changes in brain structure and function that correlate with persistent pain[1], the causal relationship between brain reorganization and pain persistence is unknown. Furthermore, changes that precede and thus predict the transition to chronicity have yet been identified[2, 3].

We studied subjects following an episode of sub–acute back pain (SBP) lasting 4–16 weeks, with no prior back pain for at least one year. Brain scans were conducted on each subject at study entry and we followed their pain and brain markers over four visits for one year. SBP patients were subdivided (20% change in pain intensity from baseline to one year, visits 1 to–4 into recovering (SBPr, n=20) and persisting (SBPp, n =19) (Fig. 1a Supplementary Fig.

*To whom correspondence should be addressed: a-apkarian@northwestern.edu.

Author contributions

M.N.B conducted the experiment, analyzed the data and prepared and wrote the manuscript; B.P. contributed to data collection and analysis; S.T. recruited subjects and conducted the experiment; K.M.H. contributed to data collection; L.H. performed data quality control; T.J.S recruited subjects and edited the manuscript; H.L.F wrote the manuscript; A.V.A. designed and supervised the experiment and wrote the manuscript.

1, for demographics see Supplementary Table 1). At baseline, SBPp and SBPr showed similar pain and mood characteristics except for the affective dimension of pain, which was significantly higher in SBPp compared to SBPr; whereas at visit 4, SBPr subjects showed decreases in most measured parameters (Supplementary Table 2a), indicating recovery from pain.

Longitudinal changes in brain structure were assessed using repeated measure ANCOVA, with gender and age as confounds. Consistent with previous reports[4], SBPp exhibited whole–brain gray matter volume decreases in time (Fig. 1b, Supplementary Fig. 2). Healthy controls, SBPp and SBPr showed some longitudinal regional gray matter density changes that were similar (Supplementary Fig. 3, 4, 5) and attributable to aging. In addition, SBPp showed significant decreases in gray matter density in bilateral striatum (focused in NAc and extending into caudate and putamen) and insula, and in left sensorimotor (S1/M1) cortex (Fig. 1c, Supplementary Fig. 3, Table 3). Region of interest analyses for right NAc and right insula showed decreased gray matter only in SBPp, longitudinally (Fig. 1d, Supplementary Fig. 4) and cross–sectionally with a significant interaction between group and visits. Similar, but less robust effects were also seen for left S1/M1 (Supplementary Fig. 4). Overall, only SBPp exhibited early, localized gray matter loss.

As NAc is part of the mesolimbic circuitry underlying reinforcement learning (the coordinates of NAc used here when tested in meta–analysis with the word “reward” gives a z–score of 15.0 for the association[5], its functional properties could illuminate the circuitry that mediates learning in pain chronification. In fact, the NAc exhibited significant positive connectivity to bilateral basal ganglia and medial prefrontal cortex (mPFC), in both SBPp and SBPr (Supplementary Fig. 5A). The contrast between SBPp and SBPr at baseline and at one year identified a strengthened mPFC connection to NAc (Fig. 2a, Supplementary Fig. 5b). The NAc exhibited significantly higher positive functional connectivity (with basal ganglia and mPFC) in SBPp at baseline and at one year (Fig. 2b). Furthermore, the number of positive connections showed a significant relation to affective pain (the only pain parameter the differed between groups at visit 1) at visit 1 and was maintained at visit 4 (Fig. 2c). NAc functional connectivity therefore differs between SBPp and SBPr, it is observed at the earliest time point available (when NAc gray matter density did not differ between groups), and persists for one year.

At baseline, the insula showed both positive and negative functional connectivity to multiple cortical regions, in both SBPp and SBPr (Supplementary Fig. 6a). At one–year follow–up, there was decreased negative functional connectivity in SBPp between insula and dorsolateral prefrontal cortex (dLPFC) and precuneus (PreCu) (Fig. 2d 2e, Supplementary Fig. 6b). This reduced functional connectivity was related positively with insula gray matter density and negatively with pain intensity (Fig. 2f). Functional connectivity of S1/M1 in relation to local gray matter density and to pain was similar to that observed for the insula, but with smaller effect sizes (Supplementary Fig. 7). These results imply that the functional reorganization of the insula and S1/M1 are coupled with gray matter changes and directly relate to the persistence of pain.

Our previous studies implicate NAc, mPFC, and their functional connectivity (mPFC–NAc) in chronic pain[6, 7]. Here mPFC–NAc functional connectivity distinguished between SBPp and SBPr at visits 1 and 4. Baseline mPFC–NAc values predicted future SBP groupings (using a separate fMRI scan, visit 1', receiver operator curves, ROC, and the areas under the curve as discrimination indices, D) best for visit 4 (with D= 0.83, $p<0.01$, unbiased estimate, Fig. 3a–c), with prediction improving at longer times from the initial inciting event. In a separate validation cohort of SBP we –examined baseline mPFC–NAc functional connectivity to predict groupings at one year and obtained a similar discrimination (Fig. 3d, Supplementary Fig. 3b). Brain–derived predictability was compared to pain parameters and to a multiple regression model incorporating mPFC–NAc, pain and drug therapy; in all cases, the mPFC–NAc functional connectivity strength was the dominant predictor of pain persistence (Supplementary Table 4a,b).

These results provide the first temporal profile of brain parameters during pain chronification. Across all measures and time points SBPr resemble healthy controls, while specific changes differentiate SBPp. Sensorimotor areas (insula, S1/M1) and a key mesolimbic (NAc) region showed decreased gray matter density in subjects with persistent pain. Insular cortex function in pain perception is well documented[1, 8, 9], and it is activated transiently with back pain in CBP[6]. This suggests a direct insular contribution to pain chronification. The role of S1/M1 in pain persistence is less certain. Sensorimotor cortical thickness recovers following effective treatment of CBP[10], and SBPp reorganization for S1/M1 was related to pain; however, postural and tactile modifications secondary to pain persistence may be causal to the observed changes. Decreased negative connectivity of the insula and S1/M1 to other cortical and to thalamic targets may contribute to back pain persistence through diminished cognitive control or by directly enhancing ascending transmission.

The NAc is activated by pain predictive cues and dopaminergic inputs to NAc signal punishment as well as reward[11–13]. Furthermore, mPFC–NAc connectivity and mPFC activity at coordinates that closely match the mPFC–NAc studied here reflect the intensity of back pain[6, 7]. The mPFC encompassed rostral anterior cingulate (ACC), a region involved in human acute and chronic pain conditions[1]. Additionally, in rodents this region is necessary and sufficient for associating pain with contextual cues[14]. These observations, along with the present results, indicate that properties and changes in mPFC/ACC–NAc circuitry are critical in the transition to chronic pain.

Current ideas regarding pain chronification have focused on peripheral nerve and spinal cord reorganization[3]. Here we show that the corticolimbic mPFC–NAc connection is an accurate predictor of the transition from subacute to chronic pain. That motivation–valuation circuitry predicts pain persistence raises the intriguing possibility that, as with positive reinforcement learning, the NAc contributes to an aversive teaching signal that leads to sustained pain intensity over time following a static peripheral injury.

Online methods

Subjects

Data presented in this manuscript is part of an ongoing study in which we examine longitudinal changes in brain structure and function in SBP patients. 120 SBP patients and 31 healthy controls were initially recruited into the study. All participants were right–handed, and were diagnosed by a clinician for back pain. An additional list of criteria was imposed including: pain intensity > 40/100 on the visual analog scale (VAS) and duration < 16 weeks. Subjects were excluded if they reported other chronic painful conditions, systemic disease, history of head injury, psychiatric diseases, or more than mild depression (score > 19), as defined by Beck's Depression Inventory (BDI). Out of the all subjects recruited, 17 healthy subjects (7 females; age: mean = 37.7, S.E.M. = 1.8 years) and 39 SBP patients (20 females; age: mean = 40.9, S.E.M. = 2.3 years) and an additional 13 SBP patients (6 females; age: mean = 42.3, S.E.M. = 2.9 years; used for outcome validation) completed this study at the time of this report. Of all subjects recruited, 34 SBP and 7 healthy subjects dropped out or were removed by visit 2, 22 SBP and 1 healthy by visit 3, and 10 SBP patients by visit 4. Some SBP patients who completed the study were removed from the analysis because of missing data.

All SBP subjects were scanned as soon as possible (mean±S.E.M pain duration from injury at visit 1 = 13.15±0.65 weeks) and were followed over the next year (visit 2: 7.15±0.45 weeks; visit 3: 29.20±0.97 weeks; visit 4: 54.36±0.97 weeks; mean ± S.E.M. from visit 1). In addition, healthy controls were scanned four times at similar intervals, for demographics see Supplementary Table 1. Dates of visits are shown for all subjects in Supplementary Figure 1A.

Pain and mood parameters

For all visits SBP patients completed the short–form of the McGill pain questionnaire (MPQ). The main component of the MPQ consists of 12 sensory and 4 affective descriptors, which are used to compute the sensory and affective scores respectively. Radiculopathy scores were quantified from pain locations that patients had shaded in with pencil on the MPQ form[15]. Patients also completed the Positive Affect Negative Affect Score (PANAS), which includes 60 items and measures the two order scales for positive and negative affect. Depression scores were assessed using BDI. All questionnaires were given 1 hour prior to brain scanning. Pain and mood parameters for SBPp and SBPr and the differences between the two groups at visits 1 and 4 are presented in Supplementary Tables 2A and 2B.

Medication

Thirty–four patients primarily used acetaminophen and NSAID (ibuprofen, Motrin, Aleve, Naproxen, Tylenol). Six patients also used opiates (Vicodin or Precocet). One subject used epidural steroid shots (Tramadol), SNRIs (Effexor and pregabalin) and muscle relaxants (cyclobenzaprine). Five patients received no treatment. Patients were subdivided into early (treatment commencement prior to visit 1) or late drug (treatment commencement post visit 1). Drug consumption at each visit was quantified using the Medication Quantification Scale (MQS), which computes a scalar value representation of dosage and duration of drug use.

Scanning parameters

For all participants and visits, MPRAGE type T1–anatomical brain images were acquired with a 3T Siemens Trio whole–body scanner with echo–planar imaging (EPI) capability using the standard radio–frequency head coil with the following parameters: voxel size 1 × 1 × 1 mm; TR, 2500 ms; TE, 3.36 ms; flip angle = 9°; in–plane matrix resolution, 256 × 256; slices, 160; field of view, 256 mm. fMRI images were acquired on the same day and scanner with the following parameters: Multi–slice T2*–weighted echo–planar images with repetition time TR = 2.5 s, echo time TE = 30 ms, flip angle = 90°, number of volumes = 244, slice thickness = 3 mm, in–plane resolution = 64×64. The 36 slices covered the whole brain from the cerebellum to the vertex.

Total gray matter volume estimation

Gray matter volume was determined using SIENAX. A standard FSL peripheral gray matter mask was used to limit gray matter volume estimation to the neocortex. Changes in gray matter volume across groups and visits were determined using a repeated measure ANCOVA with gender and age as confounds: Dependent variable gray matter volume, independent variables: visits for scanning (4 levels, within effects interaction); categorical predictors: Gender (2 levels), Group (3 levels); continuous predictor: Age. Post–hoc comparisons between groups were performed using Tukey's HSEM test.

Voxel based morphometry (VBM)

Regional gray matter density was assessed with VBM using FSL 4.1.4. The protocol included the following steps: first, a left–right symmetric study–specific gray matter template was built from 57 gray matter native images (19 images were randomly selected from each group to minimize size of population bias) and their respective mirror images that were all affine–registered to a standard gray matter template. The gray matter images were then linearly normalized onto this template. Finally, images were smoothed with isotropic Gaussian kernel (sigma= 4, FWHM = 10 mm).

Longitudinal changes in gray matter density were determined using a voxel–wise repeated measure ANOVA for each group separately. Changes in gray matter density were assessed using permutation–based inference to allow rigorous comparisons of significance within the framework of the general linear model with $p < 0.01$. Group differences were tested against 5000 random permutations. Significant clusters were identified using threshold–free cluster enhancement (TFCE) method, which bypasses the arbitrary threshold necessary in methods that use voxel–based thresholding and is more sensitive and interpretable than cluste–based thresholding methods[16]. Differences in gray matter density changes across group and visits were performed using a region of interest (ROI) analysis described below.

fMRI data acquisition and preprocessing

During scanning, patients used a finge–spanning device to continuously rate and log the rate of their spontaneous back pain on a scale of 0–100 in the absence of external stimulation[6]. Two functional scans were collected for each patient at visit 1. These fMRI are labeled visit 1 and visit 1' in Fig. 3.

The pre–processing of each subject's time series of fMRI volumes was performed using the FMRIB Expert Analysis Tool (FEAT, www.fmrib.ox.ac.uk/fsl) and encompassed: skull extraction using BET; slice time correction; motion correction; spatial smoothing using a Gaussian kernel of full–width–half–maximum 5 mm; non–linear high–pass temporal filtering (150 seconds). The first four volumes were removed to allow for signal stabilization. Several sources of noise were removed through linear regression. These included the six parameters obtained by rigid body correction of head motion, the whole–brain signal averaged over all voxels of the brain, signal from a ventricular region of interest, and signal from a region centered in the white matter.

Functional connectivity analysis

Functional correlation maps were produced using a well–validated method, see[17, 18]. Correlation maps were produced by first extracting the BOLD time course from a predetermined functional region of interest (fROI) and then computing correlation coefficient between its time course and the time variability of all other brain voxels. Correlation coefficients were converted to a normal distribution using Fischer's z–transform. A two–sided unpaired t–test was used to compute significant differences in correlations (Fischer z–transformed values) between SBPr and SBPp groups using a random effects analysis (z–score > 3.0, cluster threshold $P < 0.01$, cluster–based corrected for multiple comparisons).

Region of interest (ROI) analysis

Anatomical regions of interest (aROI) were defined from the VBM longitudinal analysis and encompassed all statistically significant voxels within an anatomical defined region of the Harvard–Oxford Structural Atlas (Supplementary Figure 4). The gray matter density for a given aROI was determined by averaging the gray matter density for all voxels within the given ROI. Differences in gray matter density across groups and visits were determined using a repeated measure ANCOVA with gender and age as confounds (same design as used for whole brain gray matter volume).

Functional regions of interest (fROI) were also determined from the VBM longitudinal analysis and were defined as 10 mm spheres centered on the voxel showing greatest longitudinal gray matter density change for each of the right NAc (x = 10, y = 12, z = −8), right INS (x = 40, y = −6, z = −2) and left S1/M1 (x = −32, y = −34, z = 66). An additional fROI within the mPFC (x = 2, y = 52, z = −2) was defined from the right NAc functional connectivity contrast map (SBPp > SBPr). The number of positives and negatives links for a given ROI were computed by 1) transforming functional connectivity maps of an ROI into standard MNI space and 2) counting the number of voxels in the whole brain with $z(r) > 0.25$ (positive links) or $z(r) < -0.25$ (negative links). Differences in number of positive and negative links across groups and visits were determined using a repeated measure ANCOVA with gender and age as confounds (same design as for whole brain gray matter volume).

Supplementary Material

Refer to Web version on PubMed Central for supplementary material.

Acknowledgements

We thank all patients and healthy volunteers that participated in the study. The study was funded by NIH NINDS NS35115. MNB was funded by an anonymous foundation.

References

1. Apkarian AV, Hashmi JA, Baliki MN. Pain. 2011; 152:s49–s64. [PubMed: 21146929]
2. Chou R, Shekelle P. JAMA. 2010; 303:1295–1302. [PubMed: 20371789]
3. Woolf CJ, Salter MW. Science. 2000; 288:1765–1769. [PubMed: 10846153]
4. Baliki MN, Schnitzer TJ, Bauer WR, Apkarian AV. PLoS One. 2011; 6:e26010. [PubMed: 22022493]
5. Yarkoni T, Poldrack RA, Nichols TE, Van Essen DC, Wager TD. Nat Methods. 2011; 8:665–670. [PubMed: 21706013]
6. Baliki MN, et al. J Neurosci. 2006; 26:12165–12173. [PubMed: 17122041]
7. Baliki MN, Geha PY, Fields HL, Apkarian AV. Neuron. 2010; 66:149–160. [PubMed: 20399736]
8. Baliki MN, Geha PY, Apkarian AV. J. Neurophysiol. 2009; 101:875–887. [PubMed: 19073802]
9. Isnard J, Magnin M, Jung J, Mauguiere F, Garcia–Larrea. Pain. 2011; 152:946–951. [PubMed: 21277680]
10. S.e.m.inowicz DA, et al. J Neurosci. 2011; 31:7540–7550. [PubMed: 21593339]
11. Ungless MA, Magill PJ, Bolam JP. Science. 2004; 303:2040–2042. [PubMed: 15044807]
12. Seymour B, et al. Nature. 2004; 429:664–667. [PubMed: 15190354]
13. Zubieta JK, et al. J Neurosci. 2005; 25:7754–7762. [PubMed: 16120776]
14. Johansen JP, Fields HL. Nat.Neurosci. 2004; 7:398–403. [PubMed: 15004562]

Online method references

15. Chanda ML, et al. J Pain. 2011; 12:792–800. [PubMed: 21497139]
16. Smith SM, Nichols TE. Neuroimage. 2008; 44:83–98. [PubMed: 18501637]
17. Baliki MN, Geha PY, Apkarian AV, Chialvo DR. J Neurosci. 2008; 28:1398–1403. [PubMed: 18256259]
18. Fox MD, et al. Proc. Natl. Acad. Sci. U.S.A. 2005; 102:9673–9678. [PubMed: 15976020]

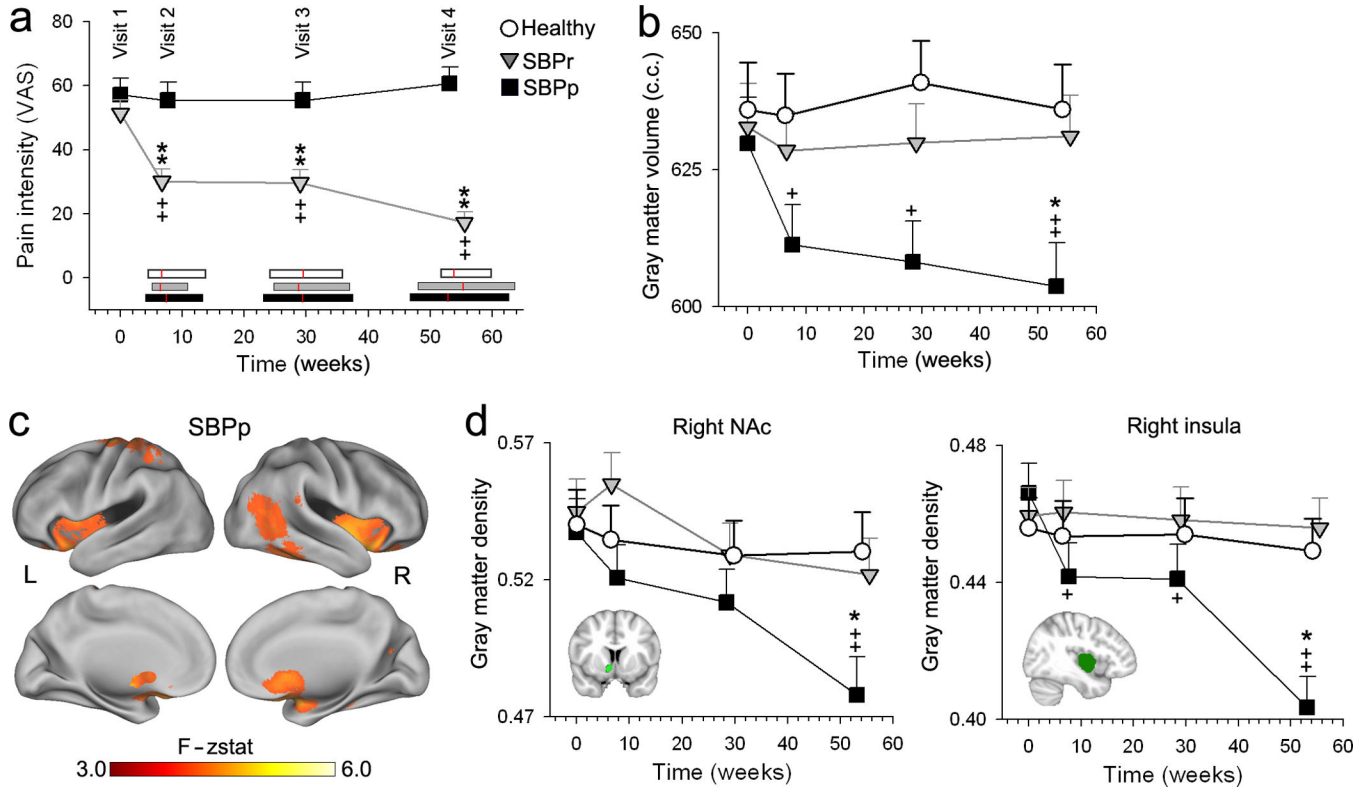

Fig. 1. Changes in global and regional gray matter density over 1 year

(**a**) Recovering SBP patients, SBPr (in contrast to persisting, SBPp) exhibited decreases in pain intensity with time. Horizontal bars represent range of times for each visit in each group (SBPp, black; SBPr, grey; healthy controls,white), red lines are the mean. Pain duration at visit 1 was not different between the groups (SBPp: mean=14.08 weeks, S.E.M.=0.97; SBPr: mean=12.36 weeks, S.E.M. = 1.04; unpaired t–test: t=1.68, p=0.16). (**b**) Gray matter volume only decreased in time in SBPp (Group*Visit $F_{6, 147}$=3.23. p<0.01). (**c**) Whole–brain voxelwise repeated measures ANOVA for gray matter density changes in time for SBPp. Regions (red–yellow) that significantly changed in gray matter density included: bilateral NAc, insula, and left S1/M1 (Supplementary Table 3). (**d**) Region of interest (ROI) analyses for right NAc and right insula showed decreased gray matter only in SBPp. The study was approved by Institutional Review Board of Northwestern University. [+p<0.05, + +p<0.01, within group comparison to visit 1; ** p<0.01 comparison to Healthy at corresponding time]. Error bars are S.E.M.

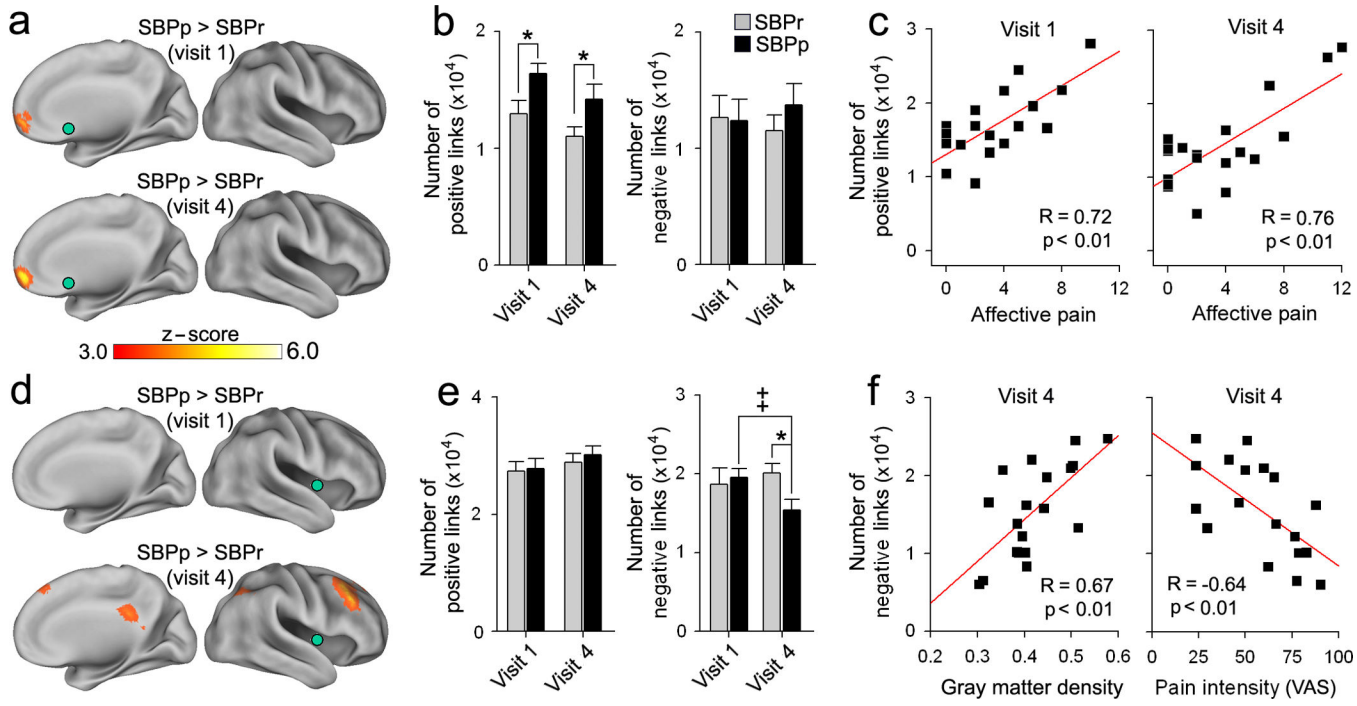

Fig. 2. Functional connectivity of NAc and insula

(**a**) Whole–brain voxelwise contrast of NAc (green) functional connectivity (links) between SBPp and SBPr. SBPp showed (red–yellow) significantly stronger positive connections between NAc and mPFC at both visits. (**b**) Average total number of voxels exhibiting positive ($z(r) > 0.25$) and negative ($z(r) < -0.25$) links to NAc. Positive functional connections were larger in SBPp at both visits. (Group $F_{1, 34}=8.80$. $p<0.01$). (**c**) In SBPp, the number of NAc positive links correlated to affective pain (computed from the affective descriptors of McGill pain questionnaire at the day of the scan) at both visits. (**d**) Whole–brain voxelwise contrast of insula (green) functional connectivity. SBPp showed decreased negative correlations between insula and dLPFC/PCC in time (Group*Visit $F_{1,34}=4.04$. $p<0.05$). (**e**) Positive and negative links to insula. SBPp showed decreased negative links at visit 4. (**f**) In SBPp and at visit 4, number of negative links to insula was related to insula gray matter density (left), and to pain intensity (right). [*$p<0.05$ in comparison to Healthy], [++$p<0.01$, within group comparison]. Error bars are S.E.M.

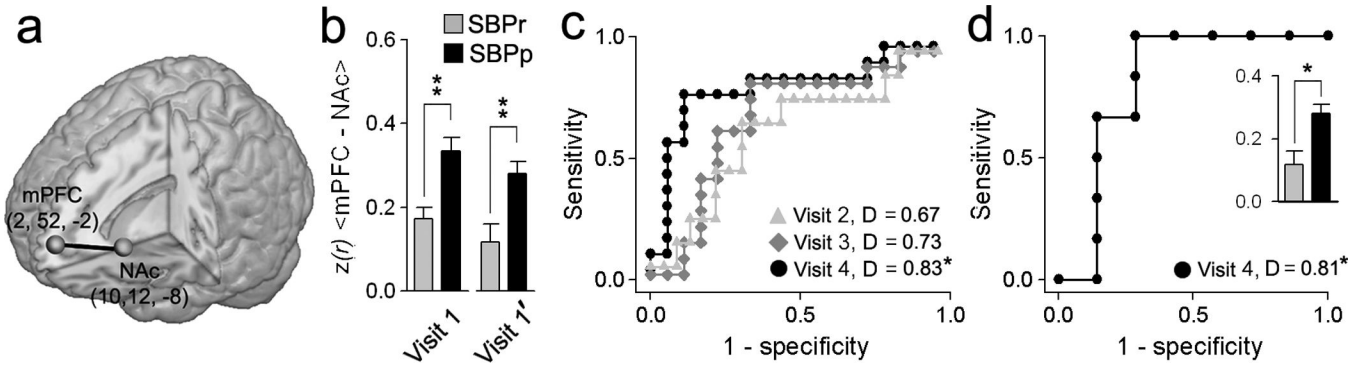

Fig. 3. mPFC–NAc functional connectivity predicts pain chronification

(**a**) Location and coordinates of the mPFC and NAc seeds used. (**b**) mPFC–NAc functional connectivity in SBPp was higher than in SBPr in separate fMRI scans. (**c**) Receiver–operator characteristic (ROC) curves and discrimination probabilities (D, area under ROC curve) for predicting pain persistence at visits 2, 3 and 4 using mPFC–NAc at visit 1' (unbiased estimate). (**d**) In a separate validation group (n=13), mPFC–NAc strengths at visit 1 (inset), and ROC and D–values of visit 1 predicting persistence of pain at visit 4. [*p<0.05, **p<0.001] Error bars are S.E.M.